

Nonadiabatic observables in β Cephei models

H. Cugier¹, W.A. Dziembowski², and A.A. Pamyatnykh^{2,3}

¹ Astronomical Institute of the Wrocław University, ul. Kopernika 11, PL-51-622 Wrocław, Poland

² N. Copernicus Astronomical Center, ul. Bartycka 18, PL-00-716 Warsaw, Poland

³ Institute of Astronomy, Pyatnitskaya 48, 109017 Moscow, Russia

Received 20 April 1994 / Accepted 26 May 1994

Abstract. Using results of linear nonadiabatic calculations for oscillations of β Cephei star models, we calculate amplitudes and phases for light, colour and radial velocity for the unstable modes of low harmonic degrees, l . The nonadiabatic observables are the amplitude ratios and the phase differences for various oscillating parameters. We construct theoretical diagrams involving these observables as well as pulsation periods and compare them with the stellar data.

Balona & Stobie (1979) showed that the diagrams based on two-colour photometric data may be used to determine the l -value of an observed mode. Our use of results of nonadiabatic calculations improves their method. We show, in particular, that the diagrams employing the satellite ultraviolet measurements are the best for discrimination between the $l = 0, 1$ and 2 cases. The clearest separation of the domains for the three l -values occurs in the diagram making use of both photometric and the radial velocity data. The observational points fall into three theoretical domains and an assignment of the l -value is unambiguous. A comparison of the theory with the observations is also made using the Period *versus* Amplitude ratios diagrams in various photometric systems. The agreement is very satisfactory and, in most cases, the l -value can be determined.

The nonadiabatic observables are useful not only to determine l but also the radial order of the observed modes as well as for constrain mean stellar parameters. As an example we consider the case of δ Ceti – a single mode β Cephei star. Our results point to the significant multicolour photometric and spectroscopic data for asteroseismology.

Key words: β Cephei stars – stars: atmospheres – stars: early-type – stars: oscillations – stars: fundamental parameters – techniques: photometry

1. Introduction

Publication of new stellar opacities calculated using the OPAL code (Iglesias et al. 1990; Rogers & Iglesias 1992) resulted in a breakthrough in our understanding of β Cephei star variability.

Send offprint requests to: H. Cugier

It has been shown that the usual κ -mechanism (Cox et al. 1992; Kiriakidis et al. 1992; Moskalik & Dziembowski 1992) acting in the zone with temperature close to 2×10^5 K may drive pulsations in these stars. The crucial new feature in the opacity was a bump caused by a large number of Fe lines. The recent results of stability surveys (Dziembowski & Pamyatnykh 1993; Gautschy & Saio 1993) for stellar models calculated with the new version of the OPAL opacities (Iglesias et al. 1992) leave no doubt that the driving mechanism has been correctly identified.

It has been pointed out that β Cephei stars are attractive targets for asteroseismology. Typically, there are several low degree modes unstable in one model and multiperiodicity is a common property of the observed variability. There is a considerable probing potential in oscillation frequencies. In particular, the measured values may be used to set constraints on the internal rotation and on the convective overshooting. The crucial step for these goals is mode identification, i.e., determination of the spherical harmonic degree, l , the azimuthal order, m , and the radial order, n , for the observed mode.

Balona & Stobie (1979) and Stamford & Watson (1981) developed methods of determination of the l -value employing data on light, colour, radial velocity amplitudes and phases. This approach was subsequently applied to β Cephei stars by several authors. In particular, Watson (1988) recommends the diagram Colour amplitude / Visual amplitude *vs.* Colour phase – Visual phase as the best discriminant of l . In this paper we investigate how the progress in our understanding of nonadiabatic pulsation properties allows to improve these methods. Having a credible linear nonadiabatic theory we may compare its prediction for the amplitude ratios and the phase differences – the nonadiabatic observables – with data for β Cephei stars. We explore how such a comparison may be used to infer the n -value of the mode and to determine the mean stellar parameters. This is particularly interesting in the case of multiperiodic objects where we deal with redundant information.

The plan of the paper is as follows. First, in Sect. 2, we briefly review behaviour of the eigenfunctions in the outer layers of stellar model. Next, in Sect. 3 we describe the method of calculation of the observable parameters which consists in fitting static atmosphere models to the dynamic interior and av-

eraging over the stellar disk. The results of calculations of the nonadiabatic observables for unstable modes with $l = 0, 1$ and 2 for selected models in the mass range $8 - 16 M_{\odot}$ are presented in Sect. 4. Using plots of different observables we discuss the best way of determining the l value and the sensitivity of the observables to mode frequency and stellar parameters. In Sect. 5 we confront the observational data for several β Cephei stars with the theoretical predictions. In Sect. 6 we discuss general significance of the nonadiabatic observables for β Cephei star asteroseismology. As specific application we consider, in Sect. 7, the case of δ Ceti.

2. Eigenfunctions of nonadiabatic oscillations

In the present work we rely on results of an oscillation property survey for Main Sequence stars in the mass range from 7 to $16 M_{\odot}$ made by Dziembowski & Pamyatnykh (1993). Readers are referred that work for a discussion of properties of the unstable modes. Here we recall basic definitions and present brief discussion of the eigenfunction behaviour in outer layers. This discussion will help us to understand approximations of the procedure.

As usual, the harmonic time dependence, $\exp(i\omega t)$, and spherical harmonic horizontal dependence, $Y_l^m(\theta, \phi)$, are assumed for the first order perturbed quantities. The real part of the eigenfrequency, $\omega = \omega_R + i\omega_I$, gives the oscillation period

$$\Pi = 2\pi/\text{Re}(\omega). \quad (1)$$

We also use the nondimensional frequency

$$\sigma = \text{Re}(\omega)/(4\pi G \langle \rho \rangle)^{1/2}, \quad (2)$$

where $\langle \rho \rangle$ is the mean density of the star and G —gravitational constant.

Since all effects of rotation are ignored the displacement of a mass element for a single mode of oscillation may be written in the following form

$$\xi(r, \theta, \phi, t) = r[y(r)Y_l^m(\theta, \phi)e_r + z(r)\nabla_H Y_l^m(\theta, \phi)]e^{i\omega t}, \quad (3)$$

where e_r is the unit vector in the r -direction and

$$\nabla_H = \left(0, \frac{\partial}{\partial \theta}, \frac{1}{\sin \theta} \frac{\partial}{\partial \phi}\right). \quad (4)$$

The relative Lagrangian pressure variation is expressed as

$$\frac{\delta P}{P} = p(r)Y_l^m(\theta, \phi)e^{i\omega t}. \quad (5)$$

In addition to the eigenfunctions $y(r)$, $z(r)$, and $p(r)$ we use here $f(r)$ which in the case of radial pulsation ($l = 0$) describes the r -dependence in the relative variation of the local luminosity. In general, f is defined as follows:

$$\frac{\delta(4\pi r^2 F)}{L} = f(r)Y_l^m(\theta, \phi)e^{i\omega t}. \quad (6)$$

The behaviour of the eigenfunctions f and p in the outer part of a typical β Cephei star model is shown in Fig. 1. The

abscissa in the plots is the decimal logarithm of total pressure in the model. The plot of the model temperature is given in the same figure. The outer boundary for the pulsation calculations is located at the minimum of the pressure distance scale ($-\frac{d \ln r}{d \ln P}$), which in the present model corresponds to the optical depth $\tau = 0.5$. The arbitrary normalization factor is selected in such a way that $\text{Re}(y) = 1$ at the outer boundary. The eigenfunctions correspond to the fundamental mode and the first overtone of the radial pulsation. We emphasize, however, these eigenfunctions are only weakly l -dependent in the case of modes considered in this paper. Near the outer boundary we approximately have

$$p \approx -3\sigma^2 - 4 + \frac{l(l+1)}{3\sigma^2} \quad (7)$$

and

$$z \approx \frac{1}{3\sigma^2}. \quad (8)$$

These two equations follow from the dynamical outer boundary condition, if the Eulerian perturbation of the gravitational potential is neglected (see e.g., Cox 1980).

All the data on pulsation modes in the present paper were obtained with the code used by Dziembowski & Pamyatnykh (1993), which assumes the diffusion approximation for the radiative transfer and neglects effects of the convection. The convection does occur in narrow zones of the envelope, but it carries a negligible fraction of the total flux. This is true for all the models of β Cephei stars. This treatment of the radiative flux is sufficient for evaluation of the bolometric light amplitude, but not for monochromatic amplitudes.

The important property of the eigenfunctions shown in Fig. 1 is that they are nearly constant in the atmosphere ($\log P < 3.5$). The constancy of f extends down to $\log P \approx 5.5$, which is a consequence of the fact that the thermal time scale of the layer above is much shorter than the pulsation periods for the two modes. A sharp change in f occurs around the value $\log P = 6.75$ corresponding to $\log T \approx 5.3$. This is the metal opacity bump region where the mode driving occurs. The absolute value of f and its phase are determined in this particular region and are closely linked to the driving effect. It was therefore unreasonable to undertake project like this one before an instability of the relevant modes was found. The use of the adiabatic values for f (Buta & Smith 1979) gives a disastrous approximation. This is demonstrated in Fig. 2 where exact absolute value of f , denoted \tilde{f} , is compared with $\tilde{f} = 4\nabla_{\text{ad}} p + 2y$ —the quantity, which they use at $\tau \ll 1$ for the luminosity amplitude. The phase plotted in the same figure is defined as $180^\circ - \arg(f)$ so that it corresponds to the familiar *phase lag*, Ψ . In the adiabatic approximation we have $\Psi = 0$. Quasiadiabatic approximation for f becomes valid only at $\log P \approx 7.75$. One may see in Fig. 1 that downward from this point $\text{Im}(f) \approx 0$. One may also see that $\text{Im}(y)$ and $\text{Im}(p)$ are very close to 0 everywhere. These two latter eigenfunctions are affected very little by nonadiabatic effects.

Qualitatively, all the properties of the eigenfunctions discussed above remain valid for all models and oscillation modes relevant for β Cephei stars. The fact that the eigenfunctions are nearly constant within the optically thin layers justifies use of

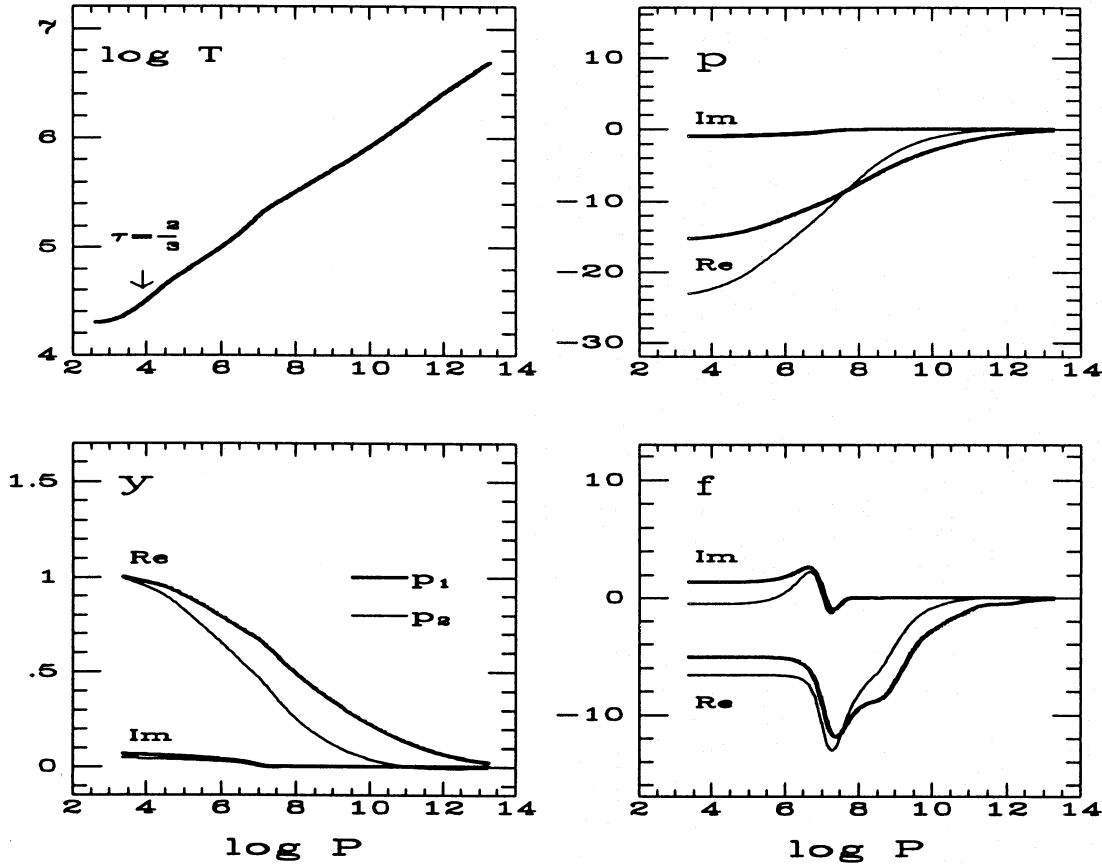


Fig. 1. Radial eigenfunctions for the fundamental mode (p_1) and the first overtone (p_2) of radial oscillations plotted against pressure in the outer part of a typical β Cephei star model. The part covers outer 55% in radius. The optical depth $\tau = 2/3$ is indicated on the plot of the model temperature. The stellar model is characterized by the following parameters: $M = 12M_{\odot}$, $\log T_{eff} = 4.37134$, $\log L/L_{\odot} = 4.28886$, $Z = 0.02$, $X = 0.7$, and the central hydrogen abundance, $X_c = 0.0818$

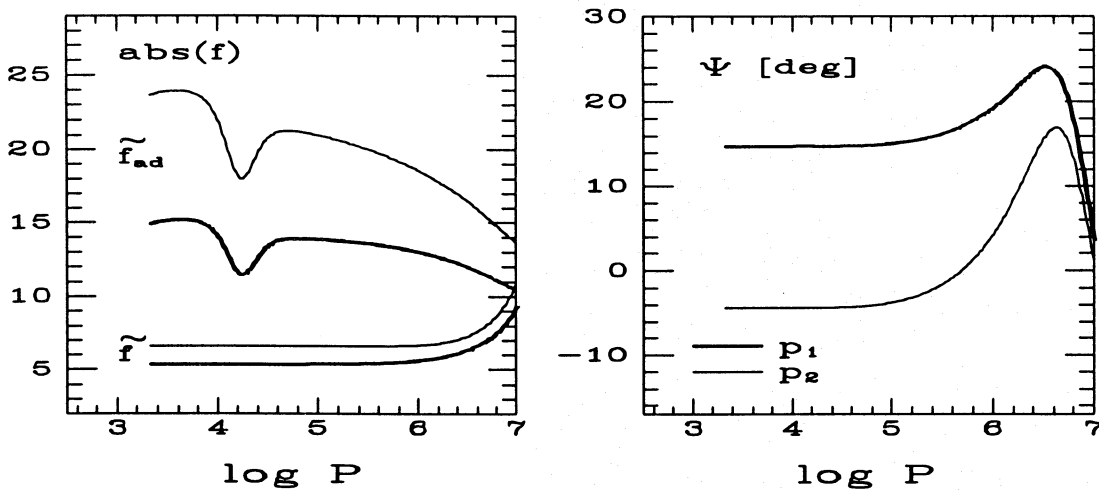


Fig. 2. Absolute value of the luminosity eigenfunction (\tilde{f}) is plotted together with the quantity \tilde{f}_{ad} , which could be used at the outer edge if the adiabatic approximation were valid. The true phase lag $\Psi = 180^{\circ} - \text{Arg}(f)$ is also plotted. The modes and the model are the same as in Fig. 1, but only outer 5% in radius is shown

static atmospheric models for evaluating of monochromatic flux changes, provided that the effects of oscillations are properly taken into account in the effective gravity.

The complex value of f is the only quantity obtained with nonadiabatic calculations that enters evaluation of the observable parameters. It depends on the mean stellar parameters T_{eff} and surface gravity g as well as on the chemical composition. It depends on dimensionless mode frequency, σ , but not directly on the l -value. The dependence on l enters only because modes of different degree have, in general, different frequencies. The strong dependence on T_{eff} and σ is illustrated in Fig. 3, where the values of \tilde{f} and Ψ are plotted for unstable modes corresponding to $l = 0$ and 2. The greater number of points in the latter case is a consequence of occurrence of unstable g-modes. The frequencies of such modes increase during Main Sequence evolution. In the models used in Fig. 3 all the unstable $l = 2$ modes have mixed character – p-mode in the envelope and g-mode in the interior. Modes are partially trapped in either of the two regions but this has no visible consequences for \tilde{f} and Ψ values.

3. Evaluation of light and radial velocity amplitudes

Following Stamford & Watson (1981) we assume that the optically thin layers may be locally approximated by plane-parallel atmospheric models. This is well justified in the present application because the radial extent of β Cephei star atmospheres is small and because we consider only modes of low l -values. We use accurate (line-blanketed) models of atmospheres taken from Kurucz (1979) for specified values of $\log T_{\text{eff}}$ and $\log g$. We include in these two parameters the effect of pulsation in the linear approximation. Expressing the stellar radius variations in the following form

$$\frac{\delta R}{R} = \epsilon \text{Re}[Y_l^m(\theta, \phi) e^{i\omega t}], \quad (9)$$

and using Eq.(5)-(7), we get

$$\frac{\delta T_{\text{eff}}}{T_{\text{eff}}} = \epsilon \frac{1}{4} \text{Re}[f Y_l^m(\theta, \phi) e^{i\omega t}] - \frac{1}{2} \frac{\delta R}{R}, \quad (10)$$

and

$$\frac{\delta g}{g} = -[3\sigma^2 + 4 - \frac{l(l+1)}{3\sigma^2}] \frac{\delta R}{R} \quad (11).$$

The last equation follows from Eq.(7) if the spacial variations of p are ignored. The term $2 - \frac{l(l+1)}{3\sigma^2}$ arises due to the relative change of the surface element, and consequently change of atmospheric mass per unit area.

For each surface element, Eqs.(10) and (11) allow us to assign a static model and calculate local specific intensity of radiation during pulsation cycle. An integration of the specific intensity variations over the stellar disk is performed using a semi-analytic method formulated by Dziembowski (1977). More details of the model calculations are given in Cugier & Boratyn (1992).

In the linear approximation, the monochromatic flux variation as seen by a distant observer may be expressed as

$$\frac{\delta \mathcal{F}_\lambda}{\mathcal{F}_\lambda^0} = \epsilon P_{l,m}(\mu_0) [(T_1 + T_2) \cos(\omega_R t + m\phi_0 + \psi) + (T_3 + T_4 + T_5) \cos(\omega_R t + m\phi_0)] \quad , \quad (12)$$

where \mathcal{F}_λ^0 denotes the flux of radiation for the equilibrium model atmosphere, $\mu_0 = \cos \theta_0$ and ϕ_0 determine the direction to the observer in (r, θ, ϕ) system, cf. Watson (1988), Heynderickx (1991) and Cugier & Boratyn (1992). Temperature effects are described by two terms T_1 and T_2 , whereas effects of the pressure changes during pulsation cycle are included in the T_4 and T_5 terms. The T_2 and T_3 terms indicate effects arising due to the sensitivity of the limb darkening parameter on temperature and gravity variations. The term T_3 corresponds to the geometrical effects. Then the flux $\mathcal{F}_\lambda = \mathcal{F}_\lambda^0 (1.0 + \delta \mathcal{F}_\lambda / \mathcal{F}_\lambda^0)$ was used to compute the magnitude variations

$$m_x = -2.5 \log \left[\int S_x(\lambda) \mathcal{F}_\lambda d\lambda / \int S_x(\lambda) d\lambda \right] - m_x^0, \quad (13)$$

for a given photometric system. $S_x(\lambda)$ is the transmission function for a passband x adopted from Matsushima (1969), Buser & Kurucz (1978), Rufener & Nicolet (1988) and Lub & Pel (1977) for the Strömgren, UBV , Geneva and Walraven systems, respectively. In the analysis we also included monochromatic magnitude variations at 150 nm. At this wavelength region the main pressure effect described by the T_4 -term in Eq. (12) is equal to zero for T_{eff} corresponding to β Cephei stars and only geometrical and temperature effects remain to be important. This indicates that the observations near 150 nm would mimic the behaviour of luminosity for these stars.

In Dziembowski's (1977) approach, the mean radial velocity variation follows from the integration, over a limb-darkened stellar disk, of the surface velocity components seen by a distant observer:

$$\Delta V_r = \omega_R \epsilon R P_{l,m}(\mu_0) (u_{l\lambda} + \alpha_H v_{l\lambda}) \cos\left(\omega_R t + m\phi_0 - \frac{\pi}{2}\right) \quad (14)$$

The coefficients α_H , $u_{l\lambda}$ and $v_{l\lambda}$ are defined in Dziembowski (1977). The $2K$ -amplitude of the radial velocity curve calculated from this formula may be used as a good approximation of the average value of radial velocities measured at the two half-intensity points, cf. Cugier (1993).

4. Identification of the spherical harmonic degree l for an observed mode

We investigate how an improved knowledge about nonadiabatic observables f and ψ affects the method of l -identification proposed by Balona & Stobie (1979) and Stamford & Watson (1981). We limited ourself to $l = 0, 1$ and 2 because large averaging effects for higher spherical harmonic degree l make such an identification highly unlikely. Making use of the calculated amplitudes and phases we constructed different diagrams in order to search for the best discriminants of oscillation modes

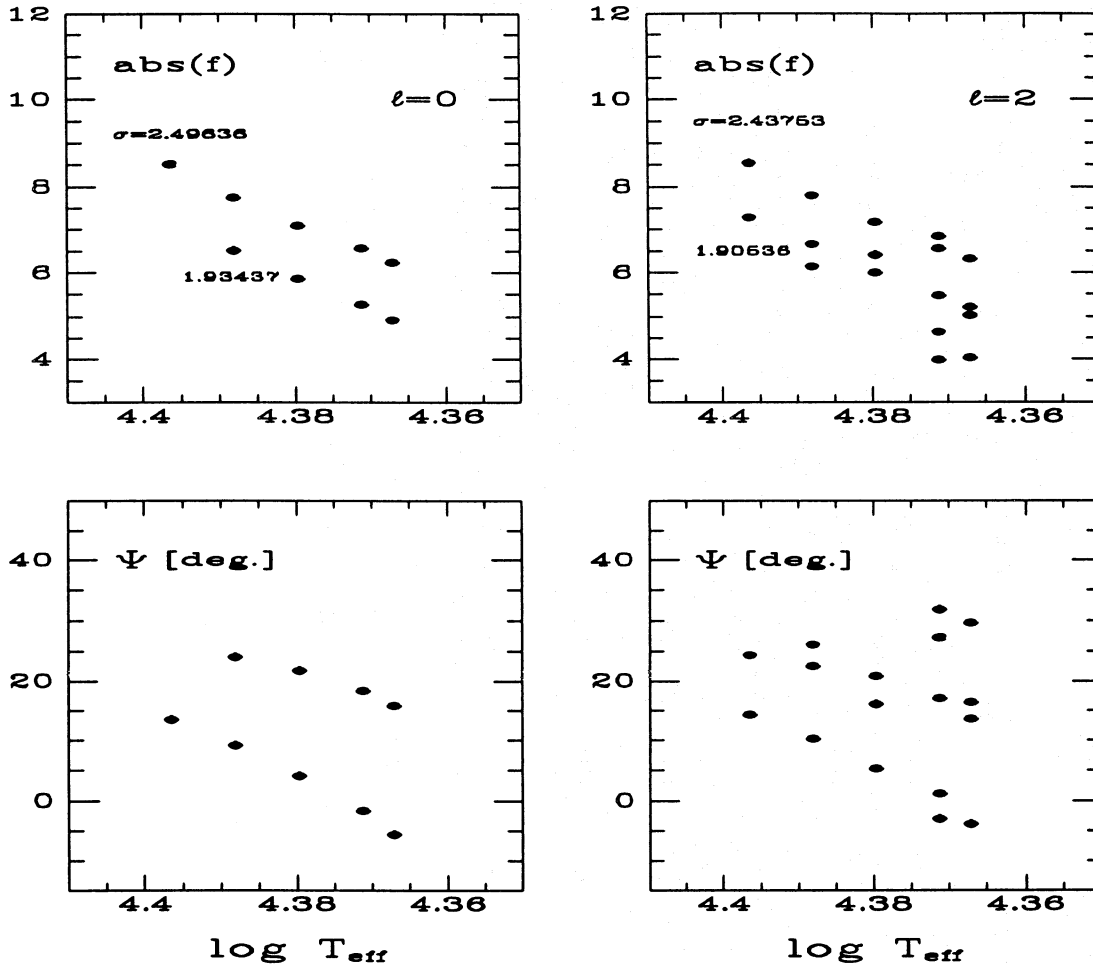


Fig. 3. Absolute values of the luminosity eigenfunction \tilde{f} and the phase lag Ψ plotted as a function of the effective temperature in a sequence of $12M_{\odot}$ star models in the expansion phase of the Main Sequence evolution. The value $Z = 0.02$ was adopted. The data for all unstable modes for $l = 0$ (left panels) and $l = 2$ in selected models are plotted. The values of dimensionless frequency σ are given at the points corresponding to the onset of particular mode instability (p_1 and p_2 for $l = 0$ and p_0 and p_1 for $l = 2$)

in β Cephei stars. Balona & Stobie (1979) demonstrated the usefulness of colour and phases data for determination of the l -values of the observed mode. Here we follow this idea but we take advantage of the fact that now we have trustworthy values of \tilde{f} and Ψ . We first considered diagrams employing only the photometric observables. By considering different diagrams we look for the most revealing photometric systems. The results are plotted in Fig. 4. The best for l determination seems the diagram with the satellite ultraviolet observations at 150 nm , where the points corresponding to different l -values occur in well separated domains. The ground based photometry may also yield an unambiguous l -values. The corresponding diagram for the Strömgren system is shown in Fig. 5. One may see that there is hardly any difference between the diagnostic value of the three ground based photometric systems.

In Figs. 4 and 5 we may see that the nonadiabatic observables, at least in the case of radial modes may be used to constrain mean stellar parameters and to discriminate between p_1 and p_2 modes. The purpose of Fig. 5 is to reveal the sensitivity

of the observables to the metal content parameter Z and to see the effect of using the OP opacities (Seaton et al. 1994) instead of the OPAL opacities used in all our standard calculations.

In Fig. 6 we show the diagram employing radial velocity amplitude, K . The separation of the domains corresponding to the different l -values is better than in the case of pure photometric observables. The greater spread of the points for the nonradial modes is another advantage of this diagram over those shown in Figs. 4 and 5.

5. Observational data

Now we proceed to analyse the observational data. We start with diagrams just found to be most useful for l -determination. In the case of multiperiodic objects we took into account the data referring to the dominant mode. Figure 7 shows the diagram K/A_V vs. A_{U-V}/A_V for stars observed at UBV photometric system. The predicted observables for unstable modes of $l = 0, 1$ and 2 are shown as dots. The numbers correspond to stars

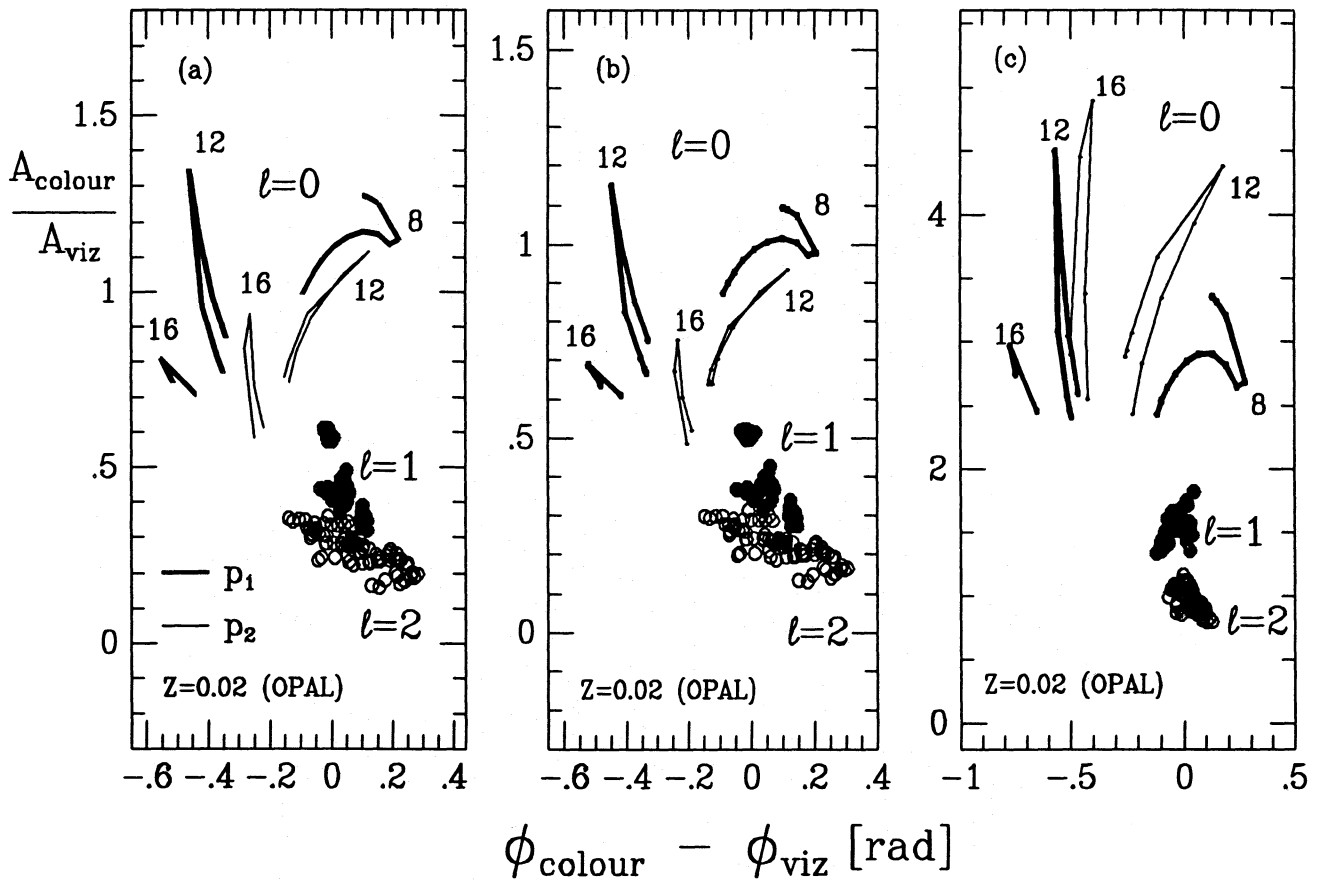


Fig. 4a-c. The colour to light amplitude ratio vs. the phase difference diagrams for the Geneva (Panel a), Walraven (Panel b) photometric systems and data employing the satellite ultraviolet observations at 150 nm (Panel c). For the $l = 0$ modes the lines correspond to the Main Sequence part of the evolutionary track where fundamental (p_1) and first overtone (p_2) modes are unstable. The values of stellar mass are indicated. The data for unstable modes with $l = 1$ and 2 in corresponding models are plotted as dots and circles, respectively

listed in Table 1. References for photometry and R.V. data are also given in this table. In all the cases shown in Fig. 7 the determination of l is unambiguous. The same is true for the stars observed at *wby* photometric system, viz., δ Cet, ν Eri, V381 Car, BU Cir and σ Sco, cf. Table 1 where l -values are listed. The photometric observables shown in our figures are known with high accuracy for the dominant mode of well observed stars (e.g., δ Cet, KP Per, V381 Car, BU Cir, σ Sco, 12 Lac and 16 Lac). In this case error bars for the photometric data are less than the size of symbols used to locate these stars in the diagrams. The published R.V. amplitudes are less accurate, but errors of the order of 30 per cent in K-values do not change our conclusion about diagnostic value of the diagram shown Fig. 7a. The diagrams corresponding to the Walraven and Geneva systems are plotted in Fig. 8 together with observed parameters for stars selected from Heynderickx's (1991, 1992) photometric survey. We omitted stars with large uncertain or conflicting periods reported in the literature. As one can see from these diagrams good overall agreement exists for all stars considered with the exception of KK Vel and δ Cet. In both diagrams (cf. Fig. 8) KK Vel is located on the left side of $l = 2$ region. The light curve for this star, as published by Cousins (1982) and Heynderickx (1991), is

distinctly non-sinusoidal but according to Heynderickx (1991) well reproduced by a sine fit with the period 0^d21569 and its first harmonic. The case when the first harmonic has a large amplitude is evidently out of scope of our model calculations. The observations of δ Cet obtained at the Walraven system (cf. Fig. 8) locate this star on the right side of $l = 0$ region, whereas *wby* and K -amplitude data discussed in Sect. 7 are in excellent agreement with the model calculations for $l = 0$. It may reflect lower accuracy of the amplitudes given by Heynderickx (1991) caused by a small number of the observations (53 data points) used in his analysis of δ Cet. We also adopted vander Linden & Sterken's (1985) data for BU Cir, which again differ from Heynderickx's ones. Generally, the number of Heynderickx's observations is mostly rather small, which may lead to misinterpretation of some stars. In particular identification of l -value for V372 Car, V836 Cen and θ Oph should be regarded as a preliminary, cf. Table 1. The same may be true for β Cephei stars belonging to NGC 3293 cluster, because values of periods are still under discussion, cf. Engelbrecht (1986), Heynderickx (1991) and Balona (1994). Heynderickx's (1991) multicolour data for the dominant modes indicate that almost all of these stars are quadrupole pulsators, cf. Fig. 8a and Table 1.

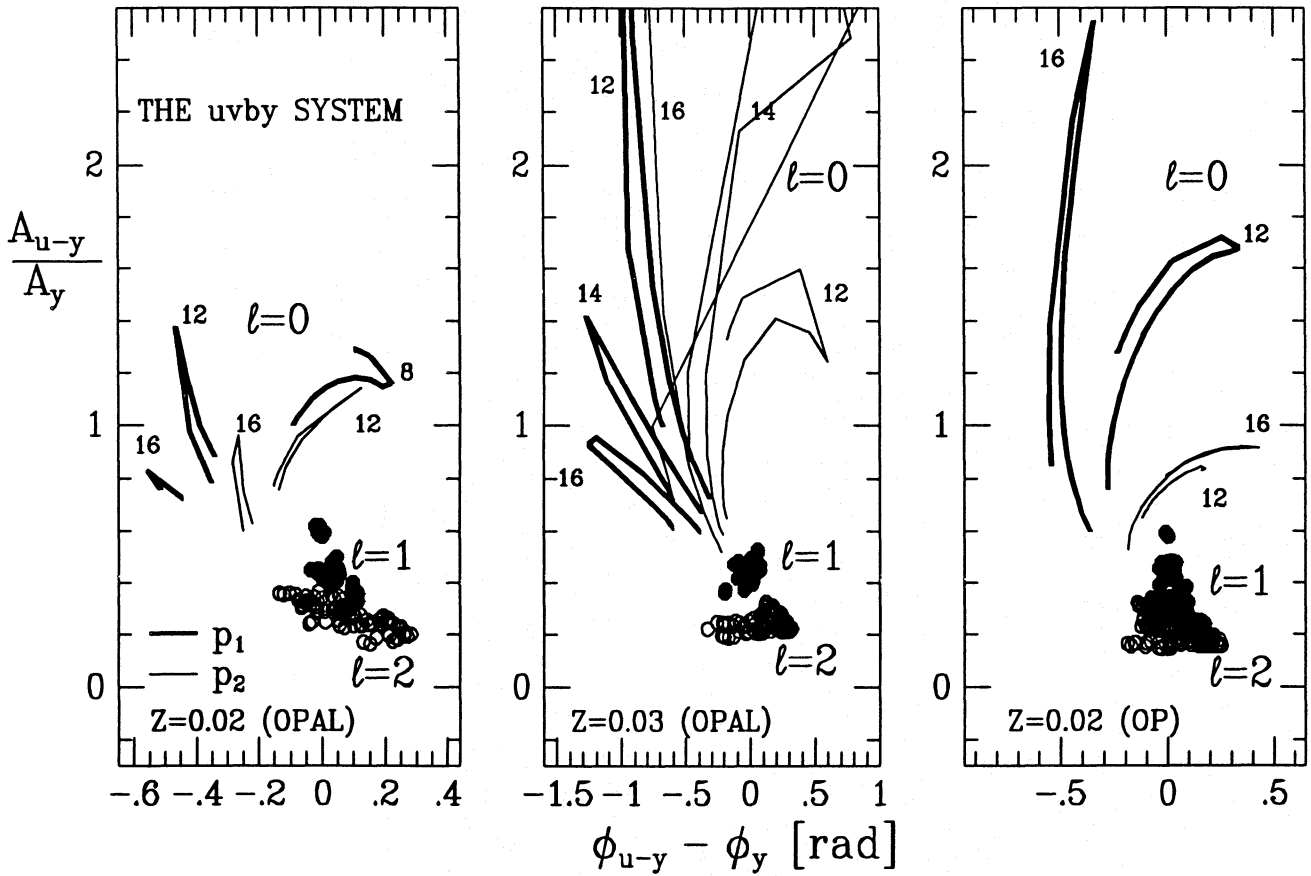


Fig. 5. Diagrams similar to those shown in Fig. 4 but obtained for the Strömgren system. The stellar models were calculated with the OPAL for two values of Z (0.02 and 0.03) and with the OP opacities for $Z = 0.02$

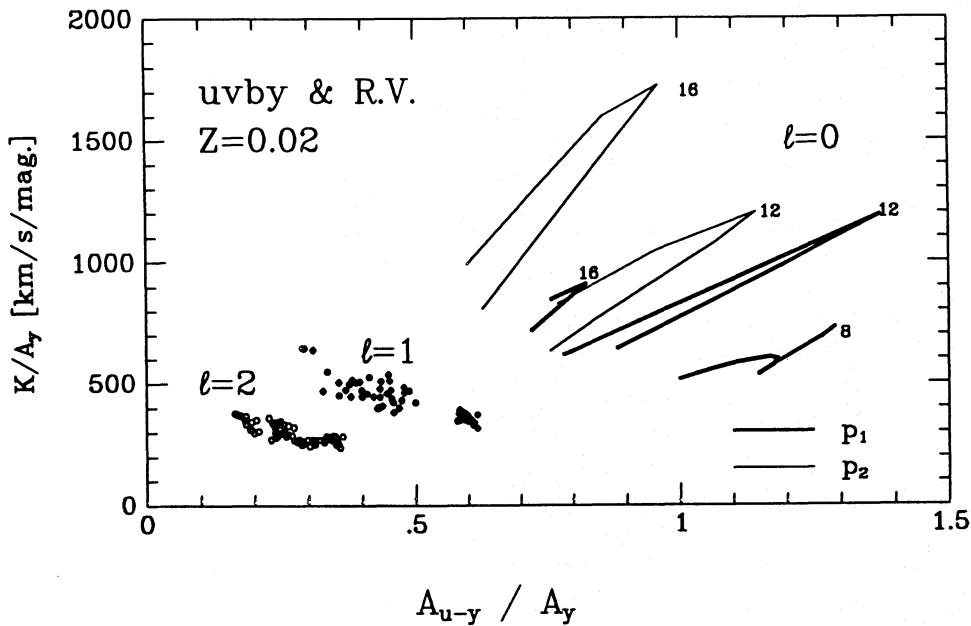


Fig. 6. The ratio of radial velocity to light amplitudes is plotted against the ratio of colour to light amplitudes

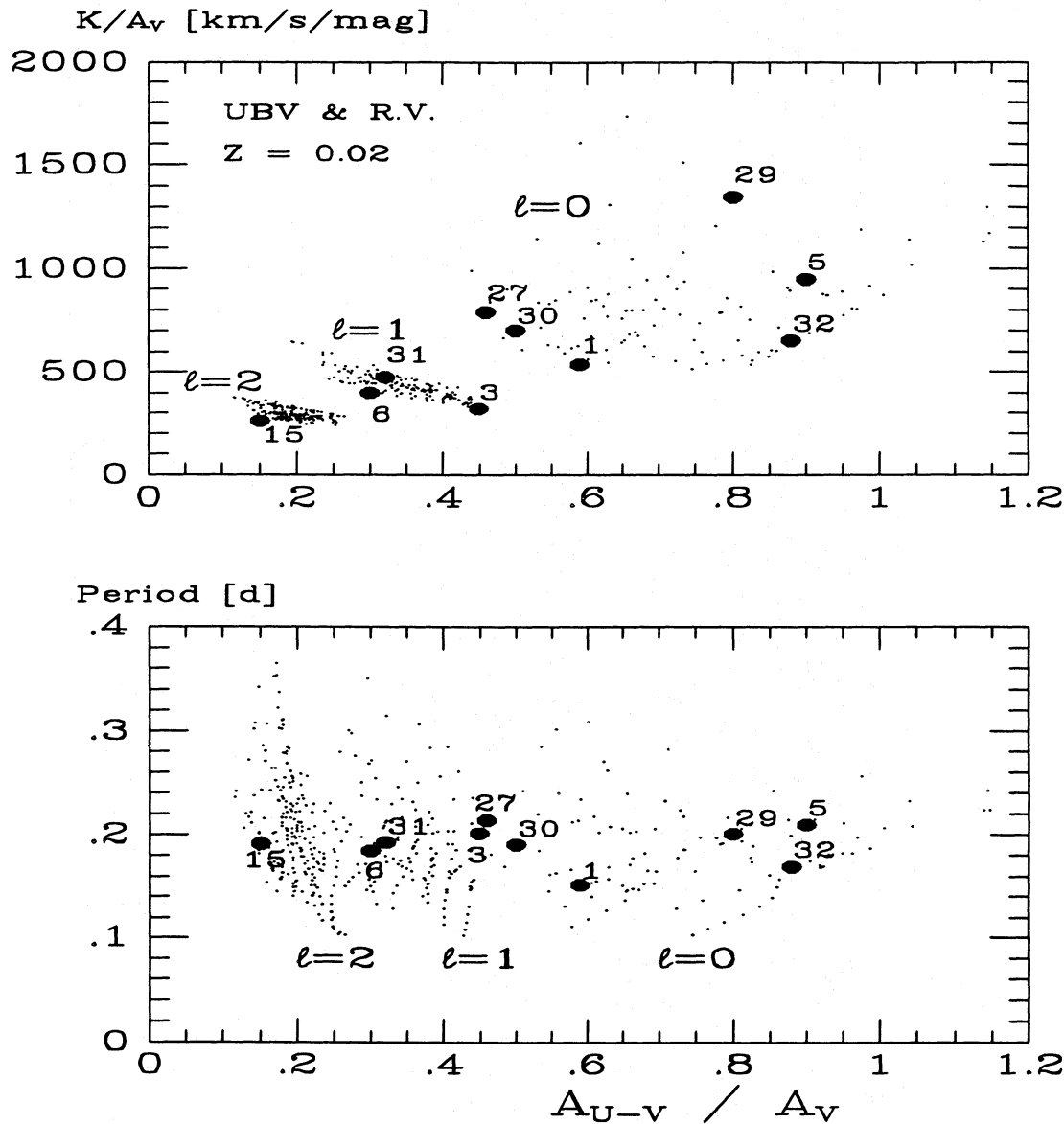


Fig. 7. **a** The ratio of radial velocity to light amplitudes is plotted against the ratio of colour to light amplitudes for unstable modes of stellar models (small dots) and dominant modes of β Cephei stars (big dots) listed in Table 1. **b** The period is plotted against the ratio of colour to light amplitudes. The small dots corresponding to different l -values occur in partially separated domains. The big dots indicate the dominant modes of β Cephei stars

The diagrams shown in this section clearly indicate that the dominant mode in a β Cephei star may be either radial or non-radial one. The identification of l is not always straightforward from published observational material, but for majority of analysed stars the same l -value is indicated from different photometric systems and different considered diagrams.

6. Nonadiabatic observables and asteroseismology

Identification of the normal modes excited in a variable star is an essential step in asteroseismology. It consists in determination of the spherical harmonic degree, l , the azimuthal order, m , and the radial order, n . So far we have focused on the l -value de-

termination. Unfortunately, the m -values cannot be directly inferred from the sparse amplitude spectra available for β Cephei stars. Determination of m is possible by means of an analysis of spectral line profile changes, as first noted by Ledoux (1951). Balona (1986a,b, 1987) developed an algorithmic method that may yield simultaneously m , l , equatorial velocity of rotation and the inclination angle. The method, however, requires high-quality spectroscopic data. (Dziembowski's (1977) modeling of radial velocity variations mentioned in Sect. 3 can be regarded as 1-st moment of a line profile in Balona's approach.)

In the double mode Cepheids and RR Lyrae stars as well as in some δ Scuti stars, the period ratio leads to a virtually unique determination of the radial order. Unfortunately, in β Cephei stars

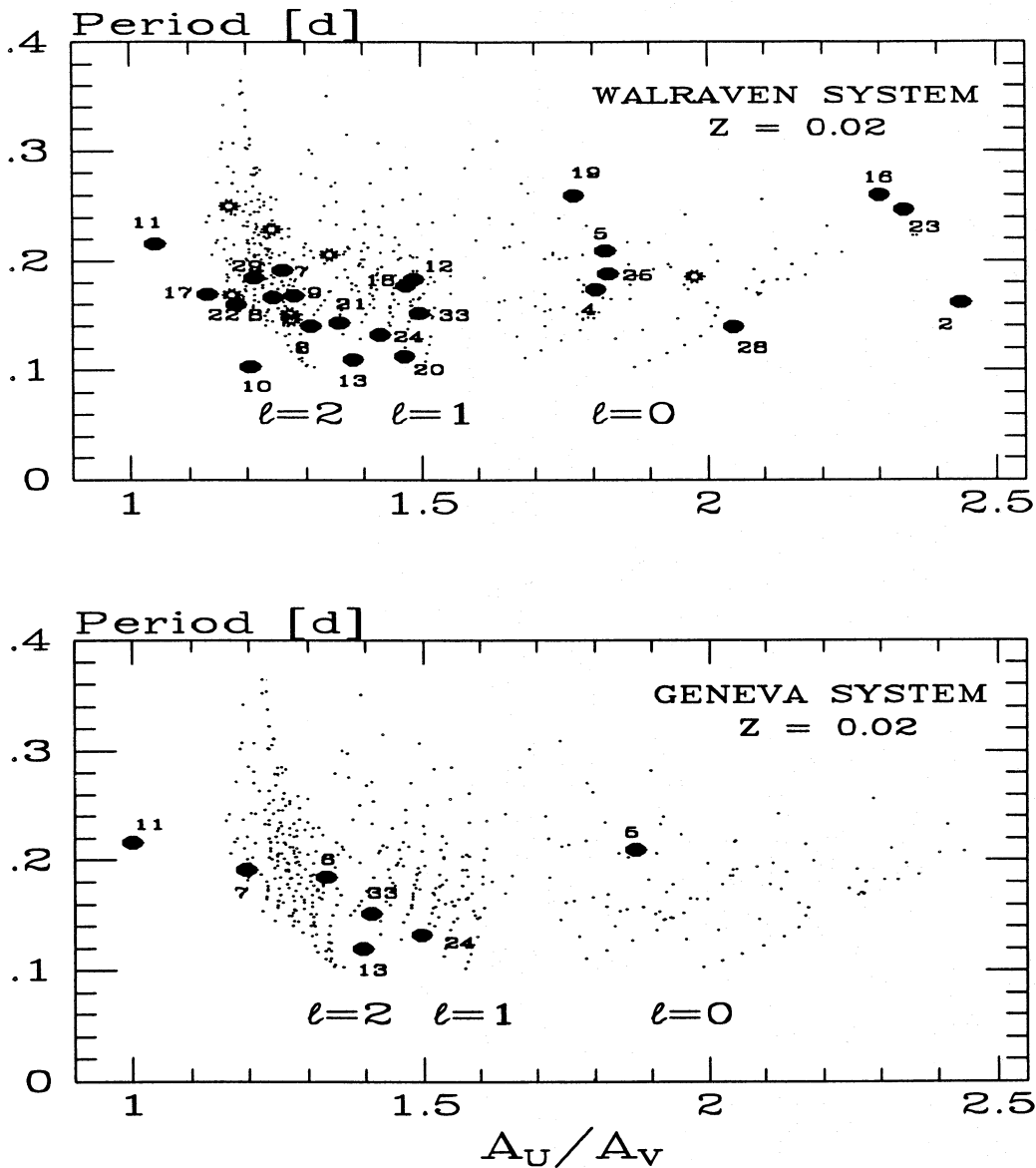


Fig. 8. The period *vs.* the ratio of light amplitudes for the Walraven and Geneva systems. β Cephei stars belonging to NGC 3293 cluster are shown as asterisks

the observed modes occur in narrow frequency ranges which preclude the presence of more than one radial mode. We should stress, however, that such a possibility is consistent with the linear theory, which predicts instability of p_1 and p_2 modes in more luminous β Cephei stars. Nonradial modes of the same l and m may have very close frequencies owing to their mixed character, as we have already discussed in Sect. 4.

Plots in Figs. 4, 5 and 6 demonstrate the usefulness of the nonadiabatic observables for the n -value determination in the case of radial oscillations. The lines corresponding to the p_1 and p_2 modes are well separated, so that with an approximate knowledge of stellar parameters, a discrimination between these two cases is possible. The situation is less favourable in the case of nonradial modes. Firstly, the points corresponding to the $l = 1$ and 2 modes cluster in rather small areas of all the diagnostic

diagrams. Secondly, the mixed character of nonradial modes complicates mode identification. Still, nonadiabatic observables may yield a useful constraint on the value of nondimensional frequency, σ , of the excited nonradial modes.

The same plots show that the nonadiabatic observables, at least in the case of radial oscillations, are also useful as a probe of the mean stellar parameters. A comparison of the diagnostic diagrams in Fig. 5 reveals a strong dependence on the metal abundance parameter, Z , as well as on the choice of the opacity data. A significant difference between the plots obtained with use of the OPAL and the OP opacities demonstrates the usefulness of the two-colour photometry of β Cephei stars for testing stellar opacities. This requires accurate T_{eff} and metal abundance values obtained from spectroscopy.

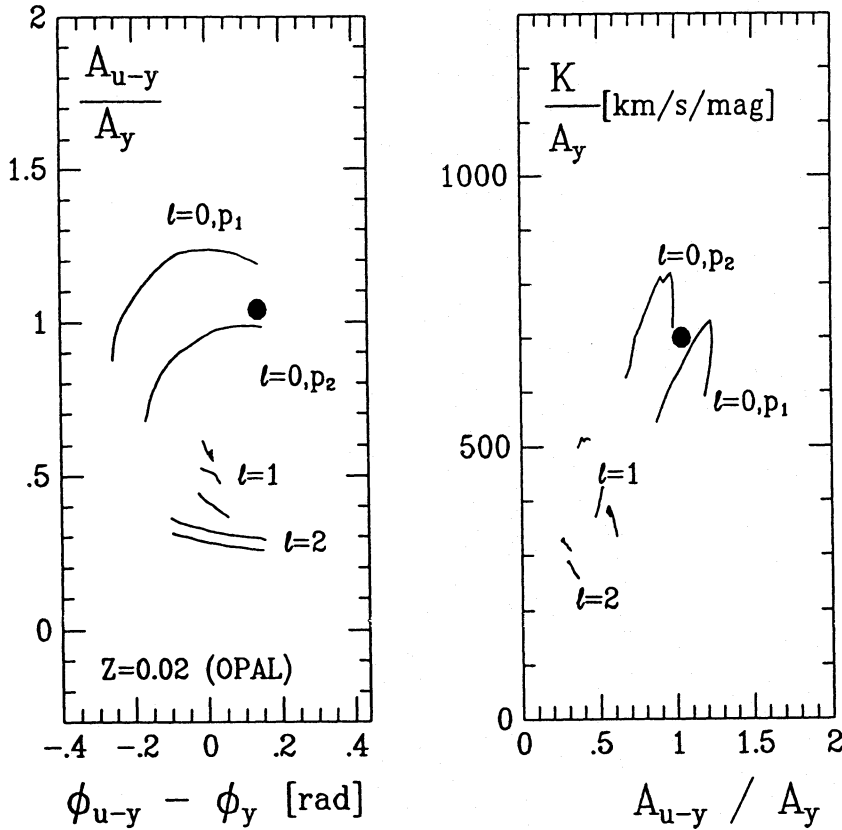


Fig. 9. **a** The colour to light amplitude ratio vs the phase difference diagram for δ Ceti. The lines correspond to unstable modes with the period exactly the same as observed for this star.

b The same as Panel **a** but the ratio of radial velocity to light amplitudes is plotted against the ratio of colour to light amplitudes

7. An encouraging example – δ Ceti

In Sect. 4 we have plotted nonadiabatic observables (cf. e.g., Figs. 4 and 5) for unstable modes having of course different periods. Figure 9 shows the same quantities but for oscillating period exactly the same as observed for δ Ceti, 0^d16114 . The observed parameters (shown as big dots) indicate that this single periodic star with almost sinusoidal light and radial velocity curves undergo radial pulsations. The observations are well described by p_2 mode of $l=0$ ($\sigma = 2.553$) corresponding to a star of $M = 10.3 M_{\odot}$ at the stage of envelope expansion during MS-phase of evolution. The further details of this solution are given in Table 2. As one can see a good agreement between observed and predicted observables exists for all photometric data as well as for effective temperature of δ Ceti.

The best fit solution shown in Table 2 predicts an increase of the pulsation period $+0.16 \text{ sec cen}^{-1}$ due to evolutionary changes of the star. The behaviour of the oscillation period of δ Ceti was studied by several authors. According to Pigulski (1992) the photometric observations together with radial velocity data yield the rate of period increase equal to $+0.28 \pm 0.02 \text{ sec cen}^{-1}$. The same value is reported by Lloyd & Pike (1984). Jerzykiewicz et al. (1988) obtained $+0.47 \pm 0.09 \text{ sec cen}^{-1}$ using only photometric (O-C) residuals, whereas the value of $+0.11 \text{ sec cen}^{-1}$ was found by Ciurla (1979) from radial velocity data. Despite of the large scatter of these data, all of them indicate an increase of the period of δ Ceti

in agreement with the expected behaviour for a star at the stage of MS envelope expansion.

8. Conclusions

Linear nonadiabatic analysis of model stellar oscillations yields, in addition to determining modes period and growth rate, two quantities that may be compared with observations. These nonadiabatic observables are evaluated from the complex eigenfunctions $y(r)$ and $f(r)$ describing variations of the radial displacement and the local luminosity, respectively. Both y and f are very nearly constant within the stellar atmosphere. Since the linear eigenfunctions may be arbitrarily normalized, there are only two real independent quantities, e.g., $\bar{f} = \text{abs}(f/y)$ and $\psi = \text{arg}(f/y)$. A conversion of \bar{f} and ψ to amplitude ratios and phase difference, that may be directly compared with observations, one has to employ a grid of realistic static models of stellar atmospheres and integrate contribution to fluxes in a selected photometric system or to the radial velocity over the stellar disk. We adopted the name *nonadiabatic observables* to denote amplitude ratios and phase difference for any pair of oscillating parameters such as light in selected filter, colour or radial velocity. We recall that such quantities are independent of the aspect and on the azimuthal order of the mode.

In our model calculations we relied on the results of the recent survey made by Dziembowski & Pamyatnykh (1993) and on the atmospheric models of Kurucz (1979). We showed that the use of the adiabatic approximation for \bar{f} gives no approx-

Table 1. Identification of the spherical harmonic degree l for the dominant mode of some β Cephei stars

No.	HD	Name	P [d]	Ref.	l
1	886	γ Peg	0.15175	1,2	0
2	16582	δ Cet	0.16114	3,4,5	0
3	21803	KP Per	0.20178	6,7,8	1
4	29248	ν Eri	0.17351	4,9	0
5	46328	ξ^1 CMa	0.20958	1,2,4	0
6	50707	15 CMa	0.18456	1,2,4	1
7	52918	19 Mon	0.19120	4	2
8	61068	PT Pup	0.16664	4	2
9	64365	QU Pup	0.16776	4	2
10	64722	V372 Car	0.10341	4	2?
11	78618	KK Vel	0.21569	4	?
12	80383	IL Vel	0.18298	4	1
13	90288		0.12023	4	1
14	92024	V381 Car	0.17730	10	2
15	111123	β Cru	0.19120	1,2	2
16	112481	V856 Cen	0.25962	4	0
17	118716	ϵ Cen	0.16943	4	2
18	126341	τ Lup	0.17737	4	1
19	129056	α Lup	0.25985	4	0
20	129557	BU Cir	0.12755	11	1
21	129929	V836 Cen	0.14313	4	1 or 2
22	145794	V349 Nor	0.15991	4	2
23	147165	σ Sco	0.23967	12	0
24	147985	V348 Nor	0.13231	4	1
25	156662	V831 Ara	0.18858	4	0
26	157056	θ Oph	0.14053	4	2 or 1
27	158926	λ Sco	0.21370	1,2	0
28	163472	V2052 Oph	0.13989	4	0
29	199140	BW Vul	0.20104	1,2	0
30	205021	β Cep	0.19049	1,2	0
31	214993	12 Lac	0.19309	13	1
32	216916	16 Lac	0.16917	14	0
33		HN Aqr	0.15218	4	1
		NGC 3293			
34		010	0.16891	4	2
35		011	0.14621	4	2
36		014	0.15153	4	2
37		016	0.25044	4	2
38		018	0.18516	4	0
39		024	0.20584	4	2
40		027	0.22880	4	2

References for photometric and R.V. data:

[1] Watson (1988), [2] Stamford & Watson (1977), [3] Jerzykiewicz et al. (1988), [4] Heynderickx (1991), [5] McNamara (1955), [6] Jerzykiewicz (1971), [7] Jarzebowski et al. (1981), [8] Struve & Zeberg (1959), [9] Kubiak & Seggewiss (1991), [10] Jerzykiewicz & Sterken (1992), [11] vander Linden & Sterken (1985), [12] Jerzykiewicz & Sterken (1984), [13] Sato (1973), [14] Jerzykiewicz (1993)

Table 2. Observables of δ Ceti

Observable	Observed	Predicted
$P =$	0.16114	0.16114 d*
$A_y =$	0.0126	0.0126 mag*
$A_u/A_y =$	2.03	1.981
$\phi_y =$	2.83	2.809 rad
$A_{u-y}/A_y =$	1.04	0.986
$\phi_{u-y} - \phi_y =$	0.14	0.140 rad
$\phi_u - \phi_y =$	0.07	0.070 rad
$2K/2A_y =$	496 – 913	732.3 km/s/mag
$2K =$	12.5 – 23.0	18.5 km/s
$l =$		0
$\sigma =$		2.553
$dP/dt =$	0.11 – 0.47	0.16 s/cen
$\log T_{\text{eff}} =$	4.336 – 4.346	4.347
Radius =		7.27 R_{\odot}
$\log g =$		3.73 [cgs]
Mass =		10.34 M_{\odot}
$\log \text{Age} =$		7.225 y
$Z =$		0.02*

* assumed

imation to correct value. In realistic models both \bar{f} and ψ depend on model parameters, changing rapidly with T_{eff} and Z . They are sensitive to nondimensional mode frequency, σ , but not to the l -value.

We reexamined diagnostic value of the diagrams showing amplitude ratio vs. phase difference for colours and luminosity for identification of the spherical harmonic degree, as it was proposed for the first time by Balona & Stobie (1979). We carried calculations for various photometric systems and we showed that employment of the satellite ultraviolet data at 150 nm is exceptionally revealing. An identification of the l value, with good photometric data should be unambiguous. The radial velocity data combined with the ground-based multicolour photometry may also be used for the same purpose. The model points corresponding to various spherical harmonic degrees occur in well separated domains and there is no ambiguity in assigning the l value to the observed modes.

Determination of the l -value is not the only use of the nonadiabatic observables. The plots shown here clearly indicate that, especially in the case of radial pulsations, the data can be used to constraint mean stellar parameters. As well, they may be used to distinguish between the fundamental and the first overtone pulsators. We believe that, in addition to precise frequency measurements, the nonadiabatic observables should be regarded as important data for asteroseismology. Thus, future efforts in this field should rely on multicolour photometry and/or employment of spectroscopic data.

Acknowledgements. This work was supported by the research grants No. 2 1185 91 01 and 2 1241 91 04 from the Polish Scientific Research Committee (KBN).

References

- Balona L.A., 1986a, MNRAS 219, 111
 Balona L.A., 1986b, MNRAS 220, 647
 Balona L.A., 1987, MNRAS 224, 41
 Balona L.A., 1994, MNRAS in press
 Balona L.A., Stobie R.S., 1979, MNRAS 189, 649
 Buser R., Kurucz R.L., 1978, A&A 70, 555
 Buta R.J., Smith M.A., 1979, ApJ 232, 213
 Ciurla T., 1979, Acta Astron. 29, 537
 Cousins A.W.J., 1982, IAU Inf. Bull. Var. Stars, No. 2158
 Cox J.P., 1980, Theory of stellar pulsation, Princeton Univ. Press, Princeton
 Cox A.N., Morgan S.M., Rogers F.J., Iglesias C.A., 1992, ApJ 393, 272
 Cugier H., 1993, Acta Astron. 43 27
 Cugier H., Boratyn D., 1992, Acta Astron. 42 191
 Dziembowski W., 1977, Acta Astron. 27 203
 Dziembowski W., Pamyatnykh A.A., 1993, MNRAS 262, 204
 Engelbrecht C.A., 1986, MNRAS 223, 189
 Gautschy A., Saio H., 1993, MNRAS 262, 213
 Heynderickx D., 1991, Ph. D. Thesis, K.U.Leuven, Belgium
 Heynderickx D., 1992, A&AS 96 207
 Iglesias C.A., Rogers F.J., Wilson B.G., 1990, ApJ 360 221
 Iglesias C.A., Rogers F.J., Wilson B.G., 1992, ApJ 397 717
 Jarzebowski T., Jerzykiewicz M., Rios Herrera M., Rios Berumen M., 1981, Rev. Mex. Astron. Astrofis. 5, 61
 Jerzykiewicz M., 1971, Acta Astron. 21, 501
 Jerzykiewicz M., 1993, Acta Astron. 43, 1
 Jerzykiewicz M., Sterken C., 1984, MNRAS 211, 297
 Jerzykiewicz M., Sterken C., 1992, MNRAS 257, 303
 Jerzykiewicz M., Sterken C., Kubiak, M., 1988, A&AS 72, 449
 Kiriakidis M., El Eid M.F., Glatzel W., 1992, MNRAS 225, 1P
 Kubiak M., Seggewiss W., 1991, Acta Astron. 41, 127
 Kurucz R., 1979, ApJS 40, 1
 Ledoux P., 1951, ApJ 114, 373
 Lloyd C., Pike C.D., 1984, Observatory 104, 9
 Lub J., Pel J.W., 1977, A&A 54, 137
 Matsushima S., 1969, ApJ 158, 1137
 McNamara D.H., 1955, ApJ 122, 95
 Moskalik P., Dziembowski W.A., 1992, A&A 256, L5
 Pigulski A., 1992, Ph. D. Thesis, Wroclaw University
 Rogers F.J., Iglesias C.A., 1992, ApJS 79,507
 Rufener F., Nicolet B., 1988 A&A 206, 357
 Sato N., 1973, A&SS 24, 215
 Seaton M.J., Yan Y., Mihalas D., Pradhan A.K., 1994, MNRAS 266, 805
 Smith M.A., 1980, ApJ 240, 149
 Stamford P.A., Watson R.D., 1977, MNRAS 180, 551
 Stamford P.A., Watson R.D., 1981, Ap&SS 77, 131
 Struve O., Zebergs V., 1959, ApJ 129, 668
 vander Linden D., Sterken C., 1985, A&A 150, 76
 Watson R.D., 1988, Ap&SS 140, 255